Fourth International Meeting on Wind Turbine Noise

Rome Italy 12-14 April 2011

Computational Aeroacoustics for Rotating Systems

S. Becker[1], J. Grabinger[1], M. Kaltenbacher[2], C. Scheit[1]
[1]Friedrich-Alexander University Erlangen-Nuremberg, Erlangen, Germany
[2]Alps Adriatic University Klagenfurt, Klagenfurt, Austria
sb@ipat.uni-erlangen.de

Abstract

The paper presents two different numerical approaches that are capable to predict the sound generation induced by turbulent flows in rotating machinery such as fans. Both methods belong to hybrid aeroacoustic methodologies, which use a previous transient CFD computation. The data from this aerodynamic simulations are then used for in-house codes solving the classical Ffowcs-Williams Hawkins (FW-H) equation (integral approach) and the inhomogeneous wave equation of Lighthill using a Finite Element (FE) method. Our second approach accounts for both the movement of flow-induced sound sources and reflection of sound waves by the casing at the same time. Both applied methodologies are computational tools for getting a better physical understanding of flow induced noise, the source distribution as well as noise propagation.

Introduction

Nowadays, noise reduction plays an important role in most product development processes and in special in the field of wind turbines. The optimization of such machines is a quite complex task, since two phenomena have to be considered: aerodynamics and aeroacoustics. Experimental studies on noise reduction mechanisms have been presented, i.e. in Neise W (1976a) and Neise W (1976b). However, due to the fact that over the past 20 years the performance of computers has strongly increased, computational techniques are now available for virtual prototyping. Therewith, the developer is able to study on the computer the complex flow, the sound generation and its propagation.

To calculate the generated and radiated sound by turbo machinery based on the unsteady flow fields, acoustic analogies are employed. The first acoustic analogy was presented in Lighthill J (1952) and Lighthill J (1954) to predict sound produced by turbulence, which was further extended in Curle N (1955) to take the influence of solid bodies into account. In FfowcsWilliams J (1969) a generalized integral formulation of Lighthill's acoustic analogy (FW-H) useful for predicting helicopter noise was presented, which is also the basis for the acoustic integral formulation used in this work. Applying FW-H acoustic analogy, a complete computational approach to predict the sound radiated by axial flow fans was presented for instance

by Maaloum A (2004) using a two-dimensional potential flow field as input for an acoustic analogy calculating only the acoustic dipole. A similar approach based on inviscid and incompressible flow was used in Jeon W (2003) for the noise prediction of a radial fan as used in a vacuum cleaner. In Moreau S (2006) they applied an approach based on the Unsteady Reynolds-Averaged Navier-Stokes (URANS) equations together with acoustic analogy and a broadband source model for the sound prediction of axial fans.

Recently, the Finite Element (FE) method has been applied to Lighthill's analogy for predicting noise radiation, e.g. from an automotive blower in Caro S (2005). In this work the blower's casing was taken into account, but the solution of Lighthill's inhomogeneous wave equation was computed only in the non-rotating system. The acoustic pressure fluctuations inside the rotor were resolved by the compressible flow computation, which requires high numerical accuracy and computational effort.

Therefore, the aim of our work is to develop numerical schemes that are able to account for the flow induced sound generation and propagation inside of rotating wind turbines. The numerical prediction tool includes acoustical effects from the movement of sound sources inside the rotor and reflection and refraction at blades of wind turbines.

Aeroacoustic Formulation

To calculate the sound pressure spectra radiated by the wind turbine impeller an approach based on FW–H and a FE-method was developed.

In a first method the acoustic pressure p' radiated by the impeller is calculated by solving the FW-H equation in the time domain. The FW-H equation is a rearrangement of the continuity and momentum equations such that an inhomogeneous wave equation is obtained. The solution to this equation can be calculated by convolution with Green's function for radiation into free field. Several different integral formulations exist in the literature. In the present work, formulation I in Farassat F (1996) is used. It can be written for a stationary, porous integration surface as

$$p'(\vec{x},t) = p'_T(\vec{x},t) + p'_L(\vec{x},t) + p'_Q(\vec{x},t), \qquad (1)$$

where p'_T denotes thickness noise, p'_L loading noise and p'_Q the quadrupole noise, which was not explicitly evaluated in the present work. Thickness and loading noise in Eq. (1) were calculated by integration over a porous integration surface S

$$4\pi p'_T(\vec{x},t) = \frac{\partial}{\partial t}\int_S \left[\frac{\rho_0 U_n}{R}\right]_{ret} dS \qquad (2)$$

$$4\pi p'_L(\vec{x},t) = \frac{1}{a_0}\frac{\partial}{\partial t}\int_S \left[\frac{L_r}{R}\right]_{ret} dS + \int_S \left[\frac{L_r}{R}\right]_{ret} dS \tag{3}$$

with ρ_0 being the density, a_0 the speed of sound at ambient conditions and R the distance between surface source and the observer position. The subscript *ret* in Eqs. (2) and (3) indicates evaluation of the integral at retarded time, and U_n and L_r are new variables as defined in Francescantonio P (1997).

$$U_i = \frac{\rho}{\rho_0} u_i \tag{4}$$

$$L_i = \left(P_{ij}\hat{n}_j + \rho u_i u_n\right) \tag{5}$$

with u_i being the velocity vector, n_j the out-ward normal vector, P_{ij} the compressible stress tensor and r_i the distance vector between the surface source and the observer position. In the case of a stationary surface the retarded time is calculated as

$$t_{ret} = t - R / a_0 \tag{6}$$

where t in Eq. (6) is the evaluation or observer time. Using Eqs. (1) to (6), one has to take simulation data from different time steps at different source positions for the evaluation of the acoustic signal. Therefore an alternative approach to Eq. (6) is used which allows taking per acoustic evaluation step simulation data from only one time step. This so-called advanced time method was presented in Caselino D (2003) and instead of Eq. (6) the advanced time or signal arrival time is used

$$t_{adv} = t + R / a_0 \tag{7}$$

Although the quadrupole noise is not explicitly calculated, all quadrupole sources inside the integration surface are implicitly taken into account by the surface integral.

In the second approach, we base our formulation on Lighthill's inhomogeneous wave equation for the sound pressure *p'*

$$\frac{1}{a_0^2}\frac{\partial^2 p'}{\partial t^2} + \frac{\partial^2 p'}{\partial x_i^{\,2}} = \frac{\partial^2 T_{ij}}{\partial x_i \partial x_j}\,, \tag{8}$$

where a_0 denotes the mean speed of sound in the acoustic medium. The Lighthill tensor T_{ij} can be approximated for the case of isentropic flow at low Mach number by

$$T_{ij} \approx \rho_0 u_i u_j \tag{9}$$

with ρ_0 being the mean density of the medium and u_i denoting the *i*-th component of the velocity vector *u*.

We obtain a weak formulation of Eq. (8), that is then suitable for discretization with the FE method, by multiplying it with a test function *w*, then integrating over the computation domain Ω, and applying Stokes' integral theorem (see, e.g. Kaltenbacher M (2010))

$$\int_\Omega \frac{1}{a_0^2}\frac{\partial^2 p'}{\partial t^2} w d\Omega + \int_\Omega \frac{\partial p'}{\partial x_i}\frac{\partial w}{\partial x_i} d\Omega - \int_\Gamma \frac{\partial p'}{\partial n} w d\Gamma = -\int_\Omega \frac{\partial w}{\partial x_i}\frac{\partial T_{ij}}{\partial x_j} d\Omega. \tag{10}$$

In this equation $\Gamma = \partial\Omega$ denotes the boundary of the computation domain, and *n* represents the outward normal vector on Γ. The boundary integral is typically set to zero at rigid obstacles.

In order to be able to account for the rotation, we impose a domain decomposition $\Omega = \Omega_1 \cup \Omega_2$ that divides the computation domain into a rotating subdomain Ω_1 and a stationary one (Ω_2). The subdomain Ω_1 rotates with an angular frequency ω, which we describe by a rotational operator r_t, so that Ω_1 can be written as a function of time

$$\Omega_1(t) = r_t \Omega_1(0). \tag{11}$$

Inside of Ω_2 we use a stationary frame of reference.

As a consequence of the domain decomposition both subdomains Ω_1, Ω_2 are discretized separately, so that we obtain two disjoint domains having two solution functions p_1, p_2, respectively.

Additionally, the decomposition gives rise to an internal boundary $\Gamma_i = \Omega_1 \cap \Omega_2$, whereas we call the exterior boundary Γ_e. We ensure exchange of sound waves between the grids of both domains (which are in general non-conforming on Γ_i) by application of the so-called Mortar method (see, e.g., Flemisch B (2006), Triebenbacher (2010)). The additional condition

$$\int_{\Gamma_i} \left(\frac{\partial p_1(r_{-t}x,t)}{\partial t} - \frac{\partial p_2(x,t)}{\partial t} \right) \mu d\Gamma = 0 \tag{12}$$

ensures continuity in the trace of both solution functions p_1, p_2 at the interface Γ_i. μ denotes a suitable test function. Furthermore, in order to achieve continuity in the flux of p_1, p_2 we introduce the Lagrange multiplier λ defined by

$$\frac{\partial \lambda}{\partial t} = \frac{\partial^2 p_1(r_{-t}x,t)}{\partial t \partial n_i} = \frac{\partial^2 p_2(x,t)}{\partial t \partial n_i}, \qquad (13)$$

where n_i denotes the outward normal vector on Γ_i. The Lagrange multiplier λ is then substituted into the boundary integral in Eq. (10).

Validation

The test case for the FW-H formulation was a design of a real impeller. First it was necessary to define the flow domain. The flow domain consisted of the impeller with all blade passages. The computational grids were generated with ANSYS ICEM 11.0 and consist of tetrahedral as well as prism elements at the walls. The grid was modelled with 2.340.567 elements (among 278.563 prism elements). These grid sizes resulted from a convergence study to assure grid independency of the solution.

To perform the numerical simulations, the commercial finite-volume-based Navier-Stokes solver ANSYS CFX 11.0 was used. The inlet boundary condition was given by the mass flow rate and the outlet boundary was defined by an opening boundary condition at ambient pressure. The rotational speeds prescribed for the impeller were obtained analytically from the torque-speed characteristic curve of the motor.

Base on the different fluid domains (stationary and rotating) a multiple-frame-of-reference numerical calculation was performed. The interface between the different frames of reference is taken to be a *Transient Rotor Stator General Connection Model*.

The turbulence model adopted is the Shear Stress Transport Model (SST) in Menter F (1993). It employs a turbulence/frequency-based model (k–ω) in the near-wall-region and a k-ε turbulence model in the bulk flow. A blending function ensures a smooth transition between the two models.

In order to get reliable data base for the validation two impellers with different wrap angle were simulated. The results were compared directly to measurements. Figure 1 shows the spectra obtained by experiment and simulation of the impeller with 150 degree wrap angle. As one can see, good agreement is obtained between for both broadband and tonal components. The slight frequency shift between the two peaks of the blade passage frequency is due to a small speed difference between simulation and experiment. To reduce the difference in the high frequency range between the experiment and simulation would need an even smaller time step in CFD and acoustic computations. The first tonal component is related to the vortex detachment, the second peak to the blade passage frequency and the third one to the second harmonic of the blade passage frequency.

In Figure 2 the sound pressure level (SPL) plotted versus the volume flow rate is shown. Both microphone measurements and simulation results for the impellers with 150 and 228 degree wrap angles are shown.

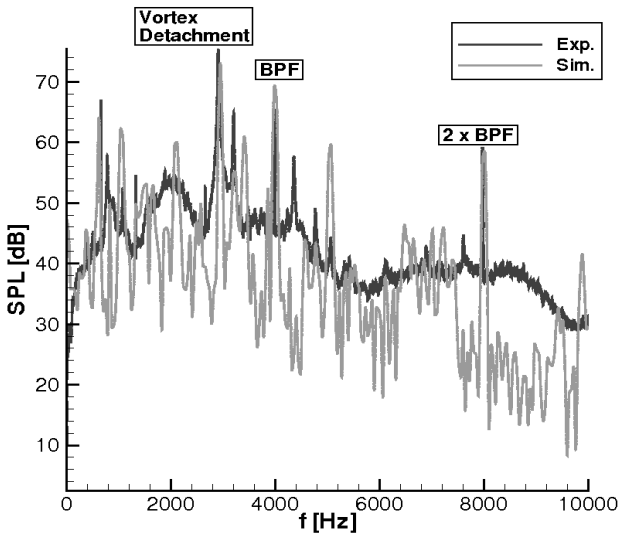

Figure 1: Radiated sound spectra from the impeller with 150 degree wrap angle; Simulation and experiment

Good agreement exists between measurement and simulation. As one can see, the impeller with 228 degree wrap angle is about 2 dB less noisy over the whole range. This result was obtained for both experiment and simulation. Figure 3 shows the frequency spectra for 150 and 228 degree wrap angle from the simulation obtained by the FW-H method.

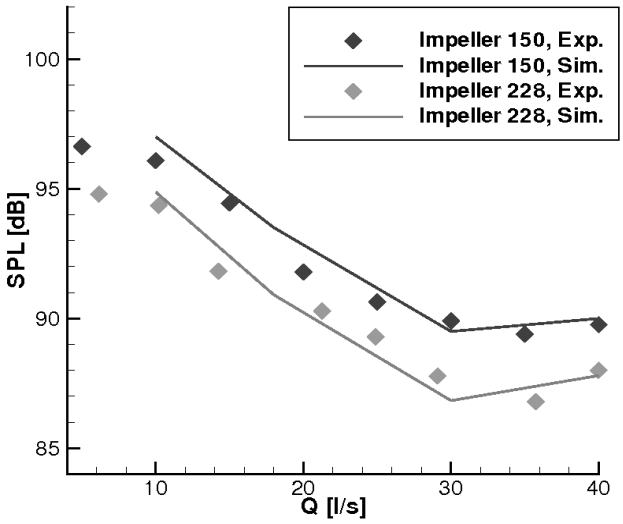

Figure 2: Sound pressure level (SPL) over volume flow rate for 150 and 228 degree wrap angle

The impeller with 150 degree wrap angle is louder than the impeller with 228 degree wrap angle over the whole frequency range.

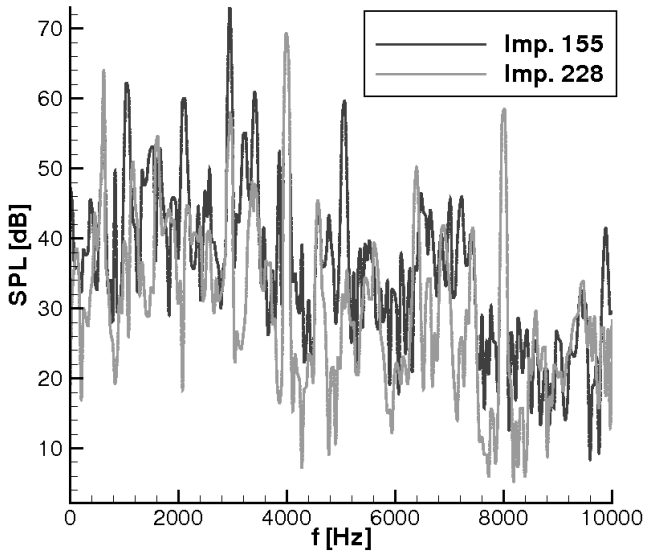

Figure 3: Simulated frequency spectra of the impellers with 150 and 228 degree wrap angle

By using the FW-H methodology it is only possible to get information of the radiated sound field. What is missing, is the acoustic source term distributions and their radiation in the near and far field. This is very important in developing efficient noise reduction tools. In such test cases we are using the new FE formulation.

The FE scheme described above is validated by applying the method to two problem settings with known analytical solution. First, we consider a simple two-dimensional case as depicted in Figure 4.

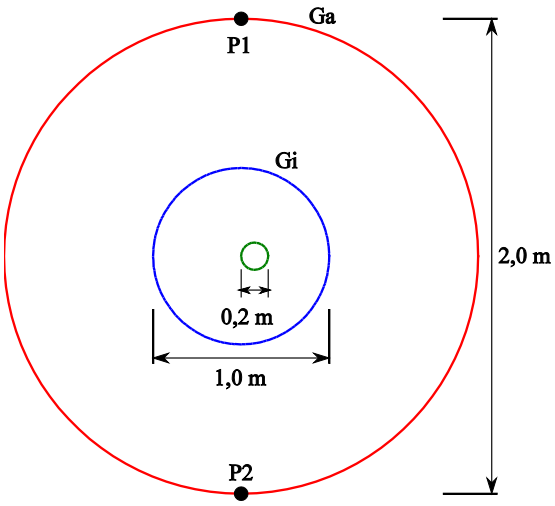

Figure 4: Test case 1- computation domain; absorbing boundary (Γ_e, —), interface between frames of reference (Γ_i, - · -), monopole source(- - -)

Inside of an air-filled volume, which rotates at 1000 rpm, we place an off-center monopole source (f = 150Hz). The rotating volume is surrounded by a volume with a stationary frame of reference. Although such a setting is completely hypothetical, it is suitable for validation of our method. We expect to observe the Doppler effect caused by the movement of the monopole source. No other effects should be observed, as there is no reflection from rigid obstacles or the outer boundary, upon which we impose an absorbing condition. Indeed the results clearly show the Doppler effect (cf. Figure 5), looking at the evolution of the sound pressure p at two observer points P1, P2 (see Figure 4).

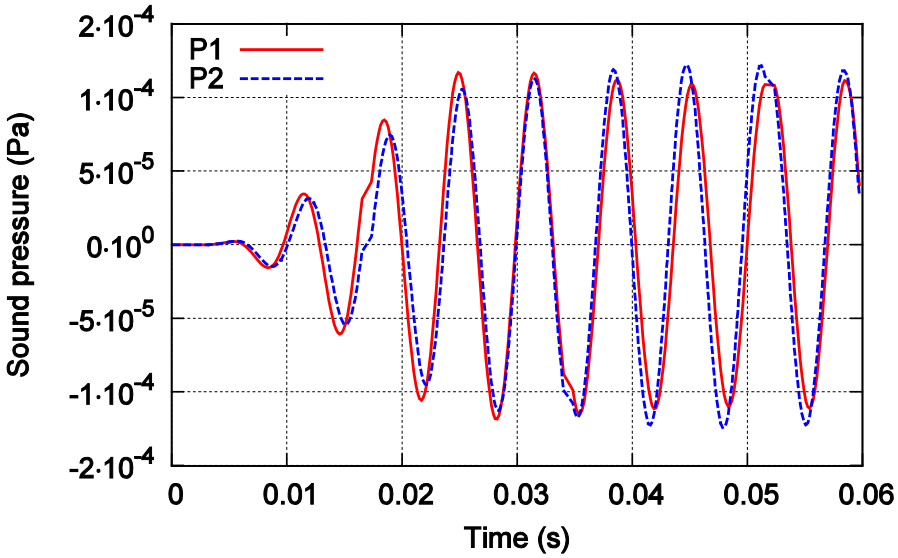

Figure 5. Evolution of sound pressure at observer points

The second validation case tests, if the method can handle more complex radiation patterns than that of a monopole. So we modify the problem setting by replacing the monopole source with a quadrupole source (now located in the center of the domain). Fig. 6 shows a snapshot of the computational domain at an arbitrary time step. One can recognize the typical quadrupole radiation pattern that gets swirled by the rotation of the acoustic source.

Conclusions

Aeroaacoustic simulations for rotating systems were carried out using a hybrid approach applying an integral formulation solving FW-H formulation and a volume discretization scheme solving Lighthill's inhomogeneous wave equation by the FE method in order to calculate the generated and radiated sound. Acoustic measurements and calculations showed good agreement, such that the approaches can be used in order to incorporate acoustic tools for the design process of wind turbines.

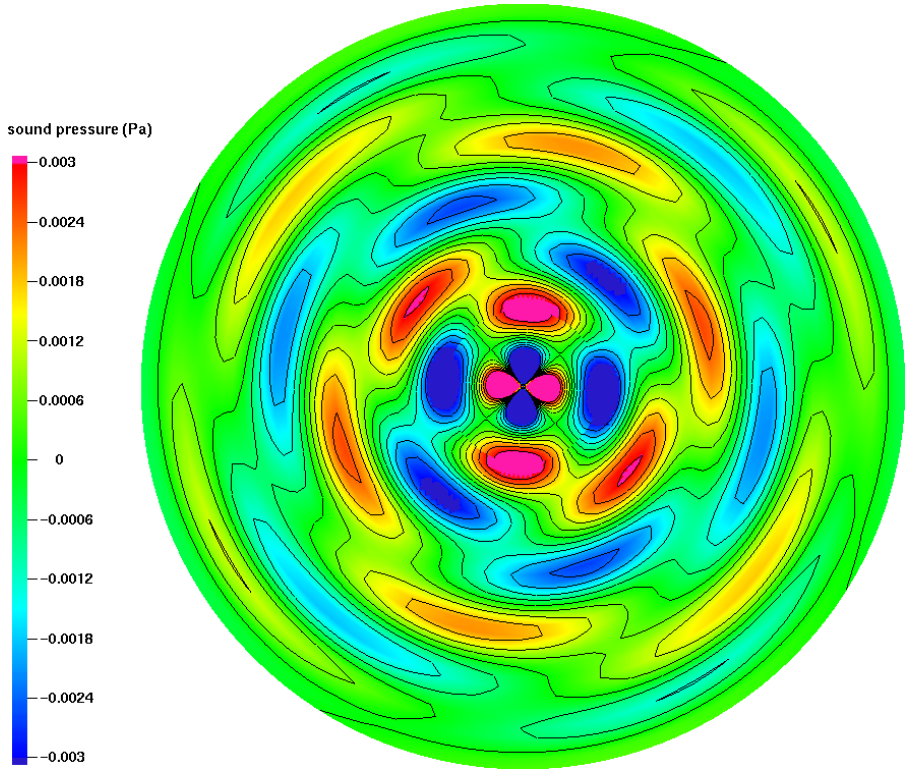

Figure 6. Contour plot of the radiation pattern of a rotating quadrupole source

With the help of the acoustic code the design of the impellers can now be done treating both the aerodynamic and aeroacoustic processes. However, one should be aware of the fact, that hydrodynamic optimized machines will not automatically be acoustically optimized. In addition to aerodynamic optimization, aeroacoustic tools should also be applied to obtain the best compromise between efficiency and noise.

References

Neise W (1976a): Neise, W, “Noise Reduction in Centrifugal Fans: a Literature Survey, Journal of Sound and Vibration, Vol. 45, No. 3, 1976, pp. 375–403.

Neise W (1976b): Neise, W. “Comments on ”Housing Effects on Centrifugal Blower Noise, Journal of Sound and Vibration”,” Vol. 46, No. 2, 1976, pp. 299–301.

Mongeau L (1993): Mongeau, L., Thompson, D. E., and McLaughlin, D. K., “Sound Generation by Rotating Stall in Centrifugal Turbomachines,” Journal of Sound and Vibration, Vol. 163, No. 1, 1993, pp. 1–30.

Lighthill J (1952): M., Lighthill, J. M., “On Sound Generated Aerodynamically I. General Theory,” Proceedings of the Royal Society, Vol. 211, No. 1107, 1952, pp. 564–587.

Lighthill J (1954): Lighthill, J. M., “On Sound Generated Aerodynamically II. Turbulence as a Source of Sound,” Proceedings of the Royal Society, 23 Feb. 1954, pp. 1–32.

Curle N (1955): Curle, N., “The Influence of Solid Boundaries upon Aerodynamic Sound,” Proceedings of the Royal Society, Vol. 231, No. A, 1955, pp. 505–514.

Ffowcs Williams J (1969): Ffowcs Williams, J. E. and Hawkings, D. L., “Sound Generation by Turbulence and Surfaces in Arbitrary Motion,” Philosophical Transactions of the Royal Society, Vol. 264, No. 1151, 8 May 1969, pp. 321–342.

Maaloum A (2004): Maaloum, A., Kouidri, S., and Rey, R., “Aeroacoustic Performance Evaluation of Axial Flow Fans based on the Unsteady Pressure Field on the Blade Surface,” Applied Acoustics, Vol. 65, 2004,pp. 367–384.

Jeon W (2003): Jeon, W.-H., Baek, S.-J., and Kim, C.-J., “Analysis of the Aeroacoustic Characteristics of the Centrifugal Fan in a Vacuum Cleaner,” Journal of Sound and Vibration, Vol. 268, 2003, pp. 1025–1035.

Moreau S (2006): Moreau, S., Henner, M., Casalino, D., Gullbrand, J., Iaccarino, G., and Wang, M., “Toward the Prediction of Low–Speed Fan Noise,” Proceedings of the Summer Program 2006, CTR Stanford, 2006.

Caro S (2005): S. Caro, P. Ploumhans, X. Gallez, R. Sandboge, F. Shakib, and M. Matthes; “A new CAA formulation based on Lighthills analogy applied to an idealized automotive HVAC blower using AcuSolve and Actran/LA”, In Proc. 11th AIAA/CEAS Aeroacoustics Conference, 23-25 May 2005, Monterey, CA, USA, number 3015 in AIAA-2005, 2005.

Farassat F (1996): Farassat, F., “Introduction to Generalized Functions with Applications in Aerodynamics and Aeroacoustics,” Technical report, NASA, April 1996.

Francescantonio P (1997), Di Francescantonio, P., “A New Boundary Integral Formulation for the Prediction of Sound Radiation,” Journal of Sound and Vibration

Vol. 202, 4, 1997, pp 491-509.

Caselino D (2003): Casalino, D., “An Advanced Time Approach for Acoustic Analogy Predictions,” Journal of Sound and Vibration, Vol. 261, 2003, pp. 583–612.

M. Kaltenbacher, M. Escobar, I. Ali and S. Becker, **“**Numerical Simulation of Flow-Induced Noise Using LES/SAS and Lighthill's Acoustics Analogy**“**, International Journal for Numerical Methods in Fluids, Vol. 63(9), pp. 1103–1122, 2010

Flemisch B (2006): Flemisch, B., Kaltenbacher, M., and Wohlmuth, B. I., “Elasto-acoustic and acoustic-acoustic coupling on nonmatching grids”, Int. J. Numerical Methods in Engineering, Vol. 67, No. 13, 2006, pp. 1791–1810.

Triebenbacher S., Kaltenbacher M., Flemisch B., Wohlmuth B., “Applications of the Mortar Finite Element Method in Vibroacoustics and Flow Induced Noise Comptations”, Acta Acustica united with Acustica2010. Vol.96, pp.536-553, 2010

Menter F (1993): Menter, F.R., “Zonal Two Equation k-w Turbulence Models for Aerodynamic Flows”, AIAA Paper 93-2906, 1993.